



Effect of titanium on the near eutectic grey iron

Moumeni, Elham; Tiedje, Niels Skat; Hattel, Jesper Henri

Publication date:
2012

[Link back to DTU Orbit](#)

Citation (APA):

Moumeni, E., Tiedje, N. S., & Hattel, J. H. (2012). *Effect of titanium on the near eutectic grey iron*. Abstract from 12th International Foundrymen Conference, Opatija, Croatia.

General rights

Copyright and moral rights for the publications made accessible in the public portal are retained by the authors and/or other copyright owners and it is a condition of accessing publications that users recognise and abide by the legal requirements associated with these rights.

- Users may download and print one copy of any publication from the public portal for the purpose of private study or research.
- You may not further distribute the material or use it for any profit-making activity or commercial gain
- You may freely distribute the URL identifying the publication in the public portal

If you believe that this document breaches copyright please contact us providing details, and we will remove access to the work immediately and investigate your claim.



Effect of titanium on the near eutectic grey iron

E. Moumeni¹, N.S.Tiedje¹ and J.H.Hattel¹

¹ Department of Mechanical Engineering, Technical University of Denmark, 2800 Kgs. Lyngby, Denmark

Abstract

The effect of Titanium on the microstructure of grey iron was investigated experimentally in this work. Tensile test bars of grey cast iron of near eutectic alloys containing 0.01, 0.1, 0.26 and 0.35% Ti, respectively were made in green sand moulds.

Chemical analysis, metallographic investigation and thermal analysis of the specimens were carried out thoroughly.

An SEM and TEM study were performed in order to observe the effect of Ti on the microstructure of the alloys in smaller scale. Furthermore, the microstructure and thermal analysis are related and discussed.

Keywords: Grey iron, titanium, SEM, TEM.

1. INTRODUCTION

The solidification and graphitization of cast iron has been attracting many scientists over the last decades, but still the mechanism is not well understood. The graphite microstructure stays the most important factor influencing the required properties of cast iron [1, 2, 3]. Therefore, its exact characterization is the only reliable indicator for mechanical properties proposed by foundries and required by customers [4].

Graphite morphology, size and distribution can be more or less efficiently controlled in the modern foundry industry using certain alloying elements and inoculation, as well as varying processing technology such as cooling rates and overheating of the melt [5]. Among all, addition of alloying elements is of the main interest in this work, whereas small amounts of alloy elements in the cast iron can improve the depth of chill, hardness and strength. Moreover, alloy elements are responsible for the amount and shape of graphite precipitated in the casting, as well as for the constitution of the iron matrix and inclusions precipitated during solidification and subsequent cooling to room temperature [6].

For instance, titanium is usually found in the grey iron as a trace element or added as an alloying element to increase strength or improve wear resistance [7]. A microstructure study showed that titanium is a relatively strong element in controlling solidification structure by increasing undercooling and thus promoting type D graphite. The

effectiveness of titanium addition depends on the base iron carbon equivalent (CE). Lerner [8] showed that changes made by Ti addition results in tensile strength improvement, but the effect depends on base iron CE. In 4.44% CE iron, tensile strength was maximized at about 0.075%Ti, while the maximum tensile strength in 4.5% CE iron took place at about 0.085% Ti. Larrañaga et.al. [9] showed that addition of appropriate sulfur and titanium contents will increase the primary austenite-to-eutectic ratio, while superfine interdendritic graphite will be produced. They demonstrated that tensile strength of grey iron of average 4% CE can be increased to 300-350 MPa, without a significant increase in hardness, which remains in the range of 185-200HB. It is worth mentioning that the influence of primary austenite dendrites on the mechanical properties of gray iron is similar to the reinforced steel bars effect in concrete or fibers in composites acting as a support frame. This means that eutectic cells will be reinforced by dendrites. [10]

The work presented in this paper represents part of a comprehensive effort to develop a fundamental understanding of the function of Ti in grey iron.

2. EXPERIMENTAL

This experimental work was carried out in the foundry of department of mechanical engineering at technical university of Denmark. The green sand moulds were made on a Disamatic 2110 moulding machine. As it is shown in Figure 1, the pattern is consisting of gating system and four tensile test samples which are different in dimensions. The thicknesses of tensile test specimens are 2, 4, 6 and 10mm.

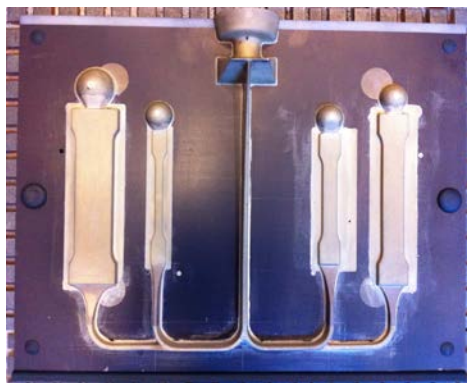


Figure 1. The pattern

The iron was melted in an induction furnace in a batch of 150 kg. The composition was near eutectic and was adjusted by addition of pig iron, cast iron returns, industrial grade silicon and steel plates. After pouring the first ladle of 30kg, ferro-titanium was added to the melt in the furnace and to reach a Ti content of 0.11%. Afterwards, the second ladle was poured with the same procedure and again ferro-titanium was added to the rest of the melt increasing the weight percent of titanium to 0.26%. The same procedure was repeated for the remaining melt so that a Ti content of 0.35% was reached. The inoculant was each time added to the melt in the pouring ladle. The composition of inoculant is presented in Table 1. The chemical composition of the melt of each ladle is presented in Table 2. The carbon equivalent is calculated according to:

$$CE = \%C + 0.317.\%Si + 0.33.\%P \quad (1)$$

Table 1-chemical composition of inoculant (weight percent)

Si	Al	Fe
52.89	0.609	Bal.

Table 2 – chemical composition analysis (weight percent)

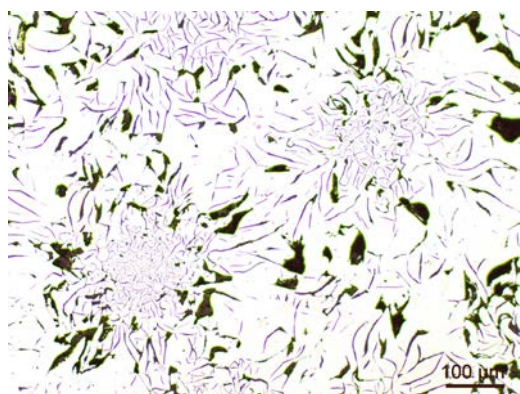
Sample	C	Si	Mn	S	P	Cu	Ti	Al	CE.
DI-1	3.34	2.57	0.16	0.015	0.030	0.04	0.01	0.006	4.16
DI-2	3.45	2.54	0.23	0.012	0.024	0.06	0.10	0.011	4.26
DI-3	3.50	2.80	0.22	0.007	0.019	0.06	0.26	0.017	4.39
DI-4	3.30	2.83	0.21	0.012	0.025	0.06	0.35	0.015	4.21

The temperature was measured in the induction furnace and the melt was superheated to 1450°C before pouring. Two “Quick Cup” samples were cast from each melt for thermal analysis. The samples for metallographic analysis were taken from the 10mm thickness specimen. The SEM images were also acquired from metallography samples. The 8mm thickness specimens were used for tensile test. Although after surface machining their thickness were lowered to 5.5mm.

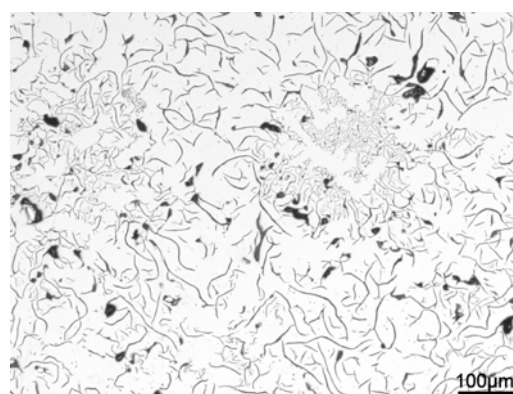
3. RESULTS AND DISCUSSION

3.1 Metallography

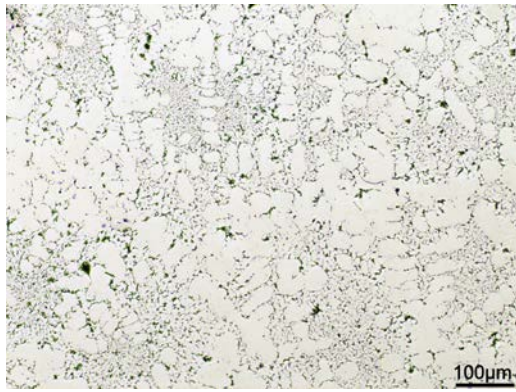
The metallographic investigation initiated by using an optical microscope. First, the images were taken after preparation without any chemical etching. As shown in Figure 2.a, in the sample no.1 the graphite is mostly type B, C and A. Sample no.2 shows finer graphite flakes in the form of type A and B (Figure 2.b). In some areas, fine graphite is formed as type D. However, in the high-Ti samples graphite is mostly formed as fine type D (Figure 2.c&d). Figure 2.b & c shows that the graphite becomes finer with increasing addition of Ti.



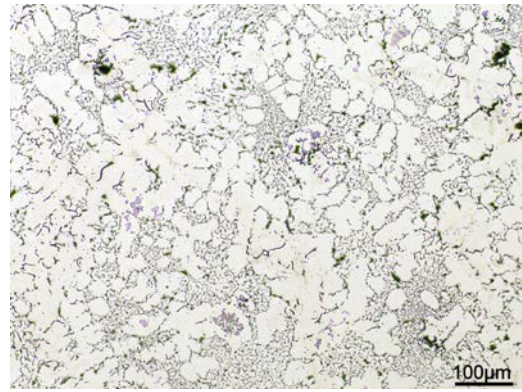
a) Sample no.1, 0.01%Ti



b) Sample no.2, 0.1%Ti



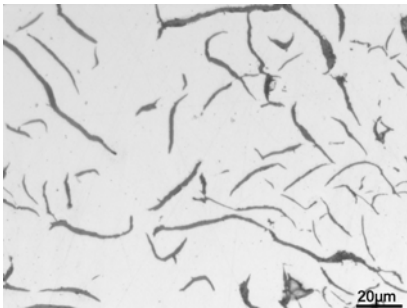
c) Sample no.3, 0.26%Ti



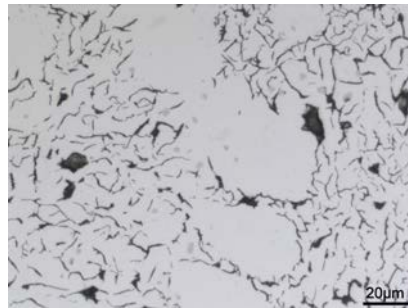
d) Sample no.4, 0.35%Ti

Figure 2 - As-cast, 100x

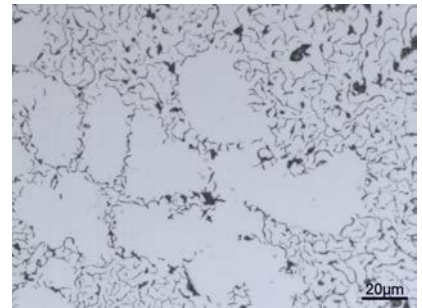
As expected, TiC inclusions were identified in the medium and high-Ti samples (Figure 3). Sample no.3 and 4 have very similar microstructure. The only difference which could be addressed is the scale of the graphite and higher number of TiC inclusions in the sample no.4.



a) Sample no.2, 0.1%Ti



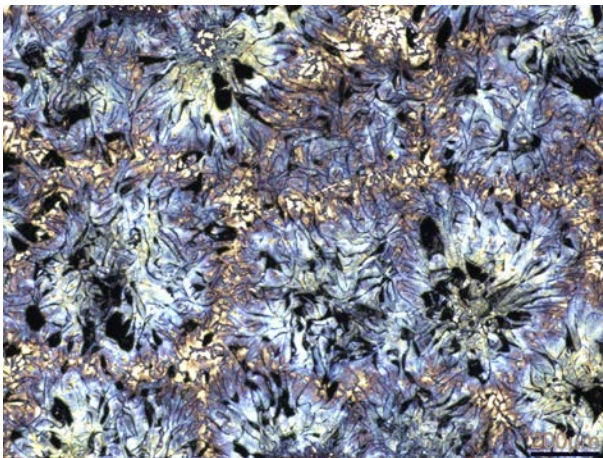
b) Sample no.3, 0.26%Ti



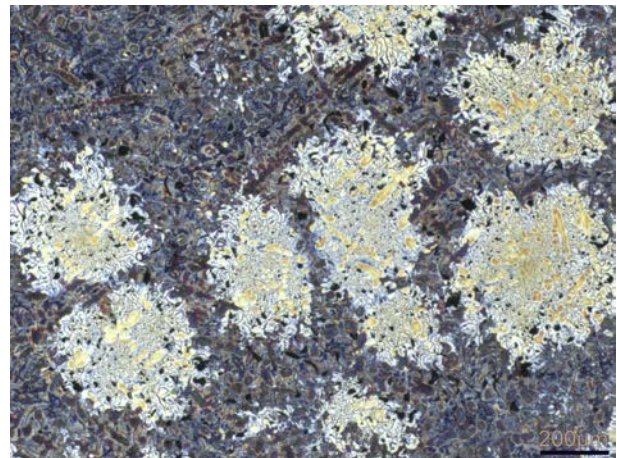
c) Sample no.4, 0.35%Ti

Figure 3- As-cast, 500x

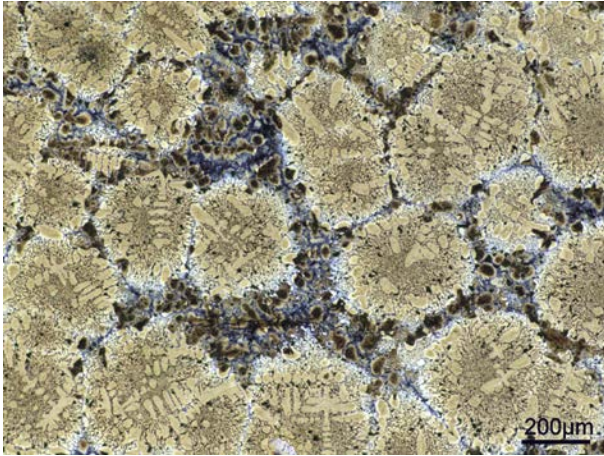
Later, the metallography samples were color etched at 70°C using the etchant 80g NaOH, 20g Picric acid in 200ml water. As it can be seen in Figure 4, addition of titanium promotes significant segregation in the microstructure. Besides, dendrites are more pronounced in the Ti containing samples.



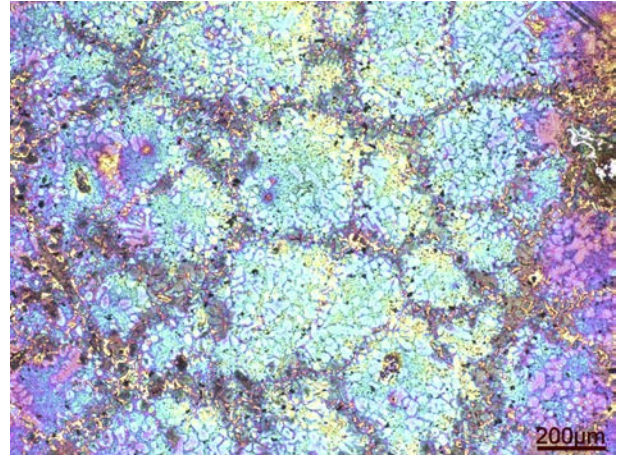
a) Sample no.1, 0.01%Ti



b) Sample no.2, 0.1%Ti



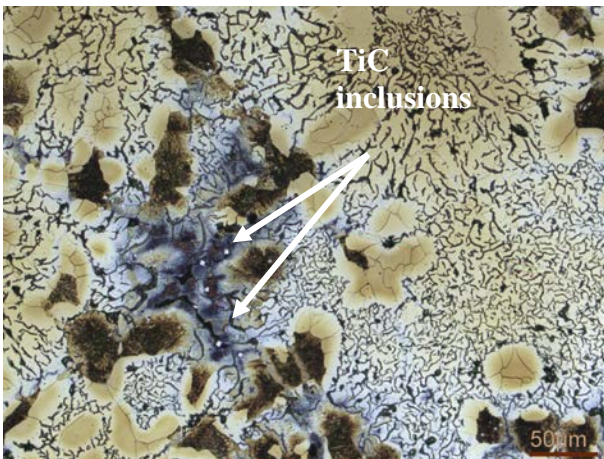
c) Sample no.3, 0.26%Ti



d) Sample no.4, 0.35%Ti

Figure 4- color etched, 50x

TiC inclusions are mostly observed at the intercellular areas (Figure 5.a), at the borders of the secondary arms of dendrites (Figure 5.b).



a) Sample no.3, 200x



b) Sample no.3, 500x

Figure 5- color etched

3.2 Electron microscopy investigation

The SEM analysis was carried out using Quanta 200 3D, dual-beam scanning electron microscope. This microscope has resolution of 50 nm at 30 kV (SE) and the accelerating voltage of 500 V to 30 kV with the capability of using a focused ion beam for removing material by milling. The in situ lift-out technique was applied to obtain TEM lamellae. A short description of this technique is explained in the subsection 3.2.1.

TEM studies (conventional and high resolution) were done using a Tecnai T20 G2 transmission electron microscope equipped to carry out chemical analysis. It has Point resolution of 0.24 nm at 200 kV and its electron source is thermionic - LaB6.

3.2.1 In situ lift-out technique

To apply in situ lift-out technique a secondary electron imaging within the chamber of a focused ion beam-SEM system is needed. Navigation to a region of interest can be performed using secondary electron (SE) imaging. After choosing the region of interest, ion beam induced platinum will be deposited on its surface and around this area will be milled by FIB milling.

The lift-out sequence starts with maneuvering the lift-out needle into position, to the side of a pre-milled section, which is only attached to the bulk sample at one point. Then the needle will be welded to the section and a cut will be made to detach the section from the bulk sample. At this point, the lamella is ready to be picked up in order to transfer to a TEM grid [11, 12]. The lift-out sequences has been shown in Figure 6.

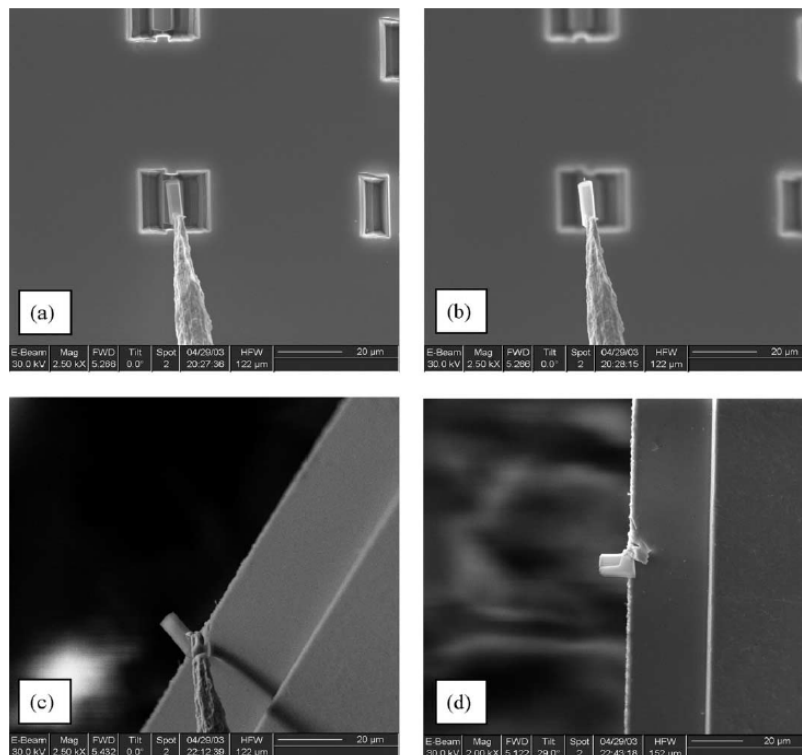
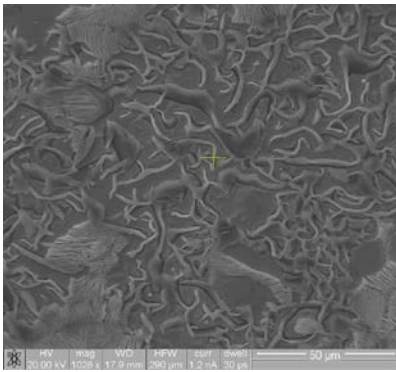


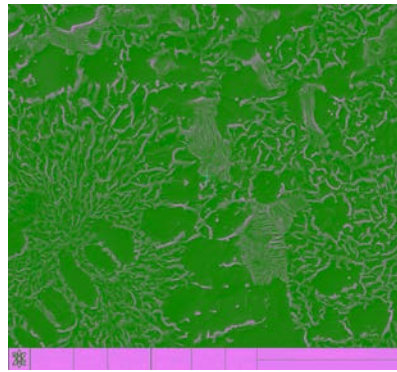
Figure 6 - SE images of (a) a cantilever shape specimen milled into the substrate with a needle Pt welded to it, (b) a wedge shaped piece of material attached to a needle raised above the sample, (c) the wedge being attached to TEM grid and (d) a wedge shape specimen attached to a grid bar into which a TEM specimen has been milled [13].

3.2.2 SEM results

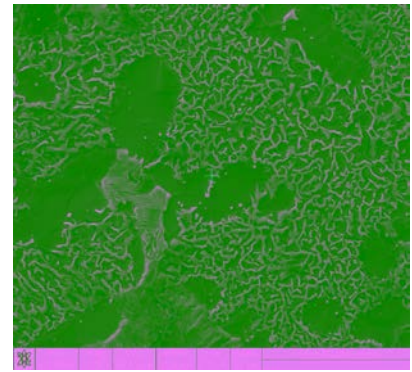
The specimens were deep etched using a 2% HNO_3 solution in alcohol for 10-15 minutes, so that the graphite and inclusions were brought forward for closer analysis. The SEM images are presented in Figure 7 & Figure 8. The trend of changes in the shape and size of graphite could be seen in these images.



a) Sample no.2, 0.1%Ti

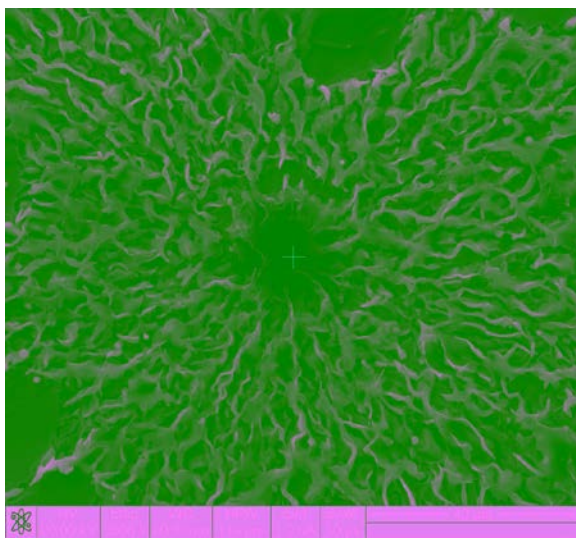


b) Sample no.3, 0.26%Ti

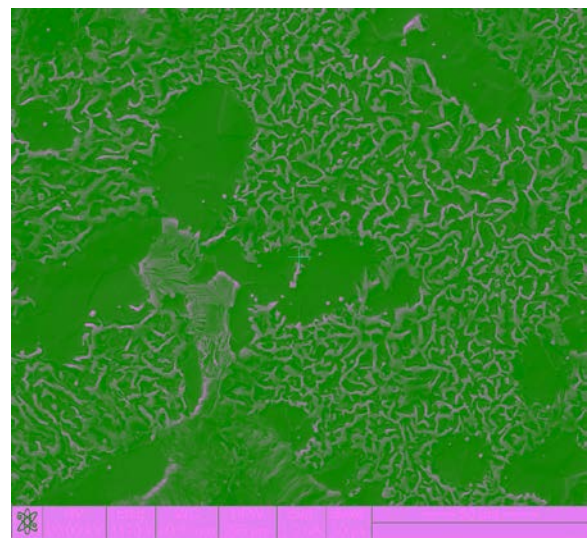


c) Sample no.4, 0.35%Ti

Figure 7- As-cast, SEM images



c) Super fine graphite



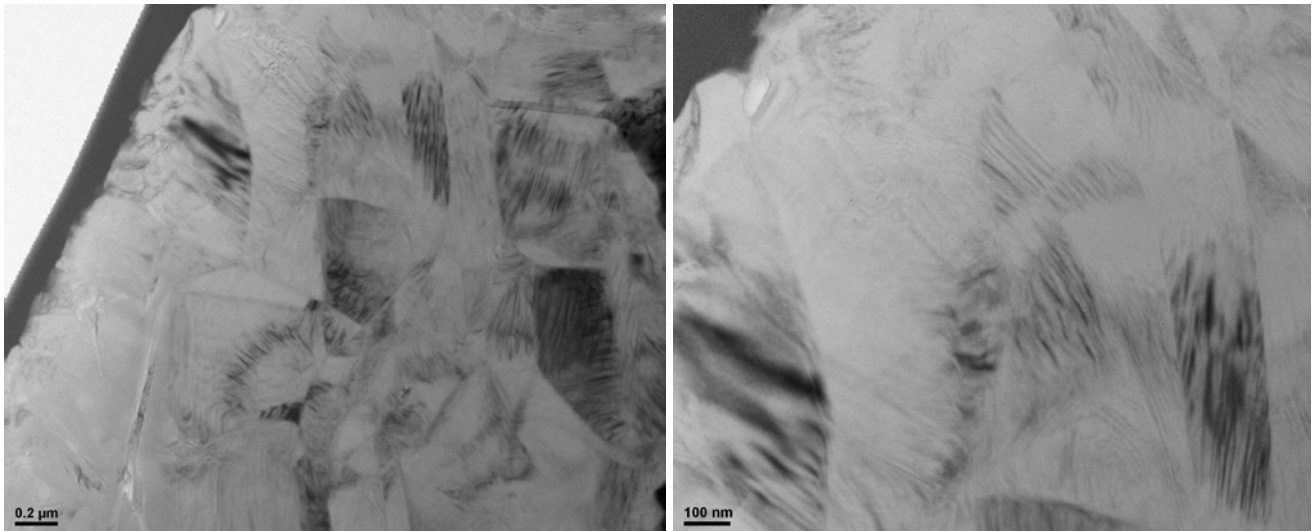
d) Super fine graphite

Figure 8- sample no.3, 0.26% Ti, SEM images

3.2.3 TEM results

A thin film sample was prepared from the fine graphite of the 0.35%Ti sample for TEM study applying the in situ lift-out technique. This sample was initially milled out of the polished sample by ion beam milling in a Helios EBS3 FIB-SEM. It was subsequently thinned for use in the TEM.

Figure 9 shows the layered structure and fine grains of graphite. Twin boundaries outline the very fine grains indicating that twinning plays an important role in the growth of the graphite lamellae.



a) Graphite lamella

b) Graphite lamella

Figure 9- TEM Images-superfine graphite

3.3 Thermal analysis

Cooling curves were obtained from melt 1, 2 and 3. As it is depicted in Figure 10, it can be seen that addition of titanium changes the shape of the cooling curve. Even though the carbon equivalent for melt 2 and 3 (as calculated using Equation 1) is marginally higher than that of melt 1, the fraction of primary austenite increases with addition of Ti to the cast iron. This shows that Equation 1 needs to be modified to correctly calculate the carbon equivalent when cast irons are alloyed with Ti. The cooling curves in Figure 9 shows that eutectic temperatures for grey irons are not changed due to the addition of Ti.

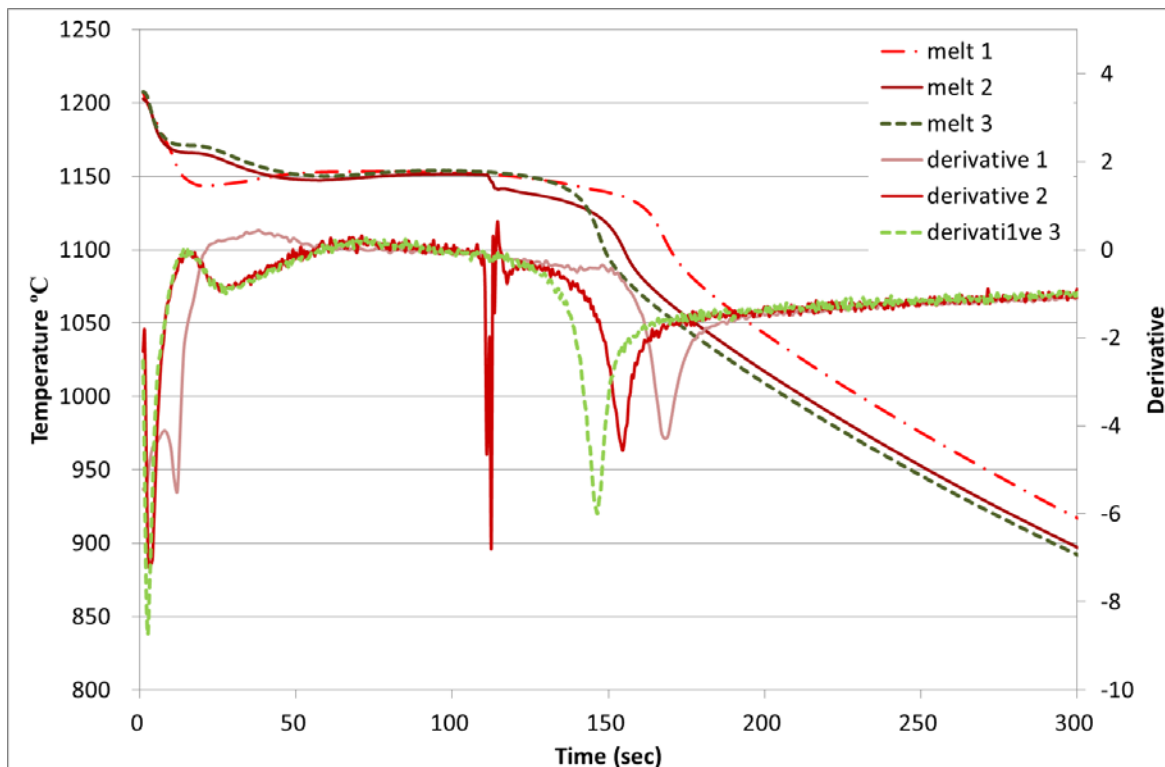


Figure 10- cooling curves and cooling rates

4. CONCLUSION

Addition of 0.1% Ti or more (up to 0.36% was tested in this work), promotes fine type D graphite and a significant segregation in the microstructure.

Titanium carbide inclusions are mostly located at the intercellular areas.

Fraction of primary austenite increases at the presence of Ti.

TEM studies shows that addition of Ti to grey cast iron makes the graphite very fine grained with twin boundaries between grains. Twin boundaries could be seen between the graphite crystals.

Cooling curves confirm the raise of formation of primary austenite dendrites with increasing the weight percent of titanium in the composition of iron.

ACKNOWLEDGEMENTS

The authors would like to thank the center of electron nanoscopy at technical university of Denmark for providing us with their equipment and knowledge. They would also like to thank Jakob S.Nielsen and Robert V.Mackay for their technical support at the foundary.

REFERENCES

- [1] Yakovlev, Metal Science and Heat Treatment, vol. 28 (1986), no. 5, p. 378–380
- [2] M. Hatate, Wear, vol. 251 (2001), pp. 885-889.
- [3] J. Chou, M. Hon and J. Lee, Mat. Science, vol. 25 (1990), pp. 1965–1972.
- [4] A. Velichko: Quantitative 3D Characterization of Graphite Morphologies in Cast Iron using FIB Microstructure Tomography, PHD Thesis, 2008.
- [5] N. Tiedje: Solidification, processing and properties of ductile cast iron, Mat Sci Tech, vol. 26 (2010), pp. 505-514.
- [6] A. Handbook, Properties and Selection: Irons, Steels, and High-Performance Alloys, Volume 1.
- [7] Z. Wang, K. Zhang, Jun Ye and C. Fan: Titanium in cast iron, Modern Cast Iron (in Chinese), vol. 2(2003), p. 31–33.
- [8] Y. Lerner: Titanium in the rapidly cooled hypereutectic gray iron, Journal of Materials Engineering and Performance, vol. 12 (April 2003), no. 2, pp. 141-146.
- [9] P. Larrañaga, J. Sertucha, A. Loizaga, R. Suárez and D. Stefanescu, "Gray Cast Iron with High Austenite-to-Eutectic Ratio, Part III," AFS transaction , 2012.
- [10] M. Chisamera, I. Riposan, S. Stan, C. Militaru, I. Anton and M. Barsto: Inoculated Slightly Hypereutectic Gray Cast Irons, ASM International, vol. 21(2012), pp. 331–338.
- [11] Lekstrom, A. McLachlan, S. Husain, D. McComb and B. Shollock: Using the in situ lift-out technique to prepare TEM specimens, IOP, 2008.
- [12] R. Langford and M. Rogers: In situ lift-out; Steps to improve yield and a comparison, Micron, vol. 39 (2008), no. 8, pp. 1325-1330.
- [13] R. Langford and C. Clinton: In situ lift-out using a FIB-SEM system, Micron, vol. 35(2004), pp. 607–611.